Volume-preserving maps with an invariant

A. Gómez
Department of Mathematics, University of Colorado, Boulder, Colorado 80309-0395 and Departamento de Matemáticas, Universidad del Valle, Cali, Colombia

J. D. Meiss
Department of Applied Mathematics, University of Colorado, Boulder, Colorado 80309-0526

(Received 10 October 2001; accepted 15 February 2002; published 22 April 2002)

Several families of volume-preserving maps on $\mathbb{R}^3$ that have an integral are constructed using techniques due to Suris. We study the dynamics of these maps as the topology of the two-dimensional level sets of the invariant changes. © *2002 American Institute of Physics.* [DOI: 10.1063/1.1469622]

Volume-preserving maps arise from the study of the flow of incompressible fluids or magnetic fields. If a volume-preserving map has a continuous symmetry, such as a rotational symmetry, then it has an invariant and the orbits are confined to surfaces. More generally, the orbits could densely cover regions with nonzero volume. Here we construct maps that have an invariant, but no (obvious) symmetry. The dynamics of these maps, while simpler than the general case, can still be chaotic on the invariant surfaces. Just as integrable systems are often used as starting points for perturbation theory, our maps provide a platform from which more general motion can be studied.

I. INTRODUCTION

In this paper we construct several families of volume-preserving maps on $\mathbb{R}^3$ that have an invariant. Some of the examples that we construct have the form,

$$f(x,y,z)=(y,z,x+F(y,z)). \tag{1}$$

Maps of this form are volume and orientation-preserving for any function F, and are diffeomorphisms whenever F is smooth. For the cases that we primarily study, F is the rational function,

$$F(y,z)=\frac{(y-z)(\alpha-\beta yz)}{1+\gamma(y^2+z^2)+\beta yz+\delta y^2z^2}. \tag{2}$$

Here there are three free parameters α, β, γ, and without loss of generality, one can suppose that the index δ can only have the values $\delta=0,\pm1$. This family of maps has an invariant, i.e., a function Φ such that

$$\Phi\circ f=\Phi. \tag{3}$$

For Eq. (2), the invariant has the form

$$\begin{aligned}\Phi(x,y,z)=&x^2+y^2+z^2+\alpha(xy+yz-zx)\\&+\gamma(x^2y^2+y^2z^2+z^2x^2)\\&+\beta(x^2yz+z^2xy-y^2zx)+\delta x^2y^2z^2.\end{aligned} \tag{4}$$

Several other examples will also be found in Sec. II, where F is rational in trigonometric or hyperbolic functions. We also construct orientation-reversing examples.

As we will see, even though each orbit of (1) is restricted to lie on the two-dimensional level sets,

$$M_\mu=\{(x,y,z):\Phi(x,y,z)=\mu\}, \tag{5}$$

they exhibit the full complexity expected for two-dimensional, area-preserving maps.

One motivation for the study of these systems is an attempt to generalize results known for two-dimensional, conservative systems, i.e., area-preserving maps. Such maps typically exhibit chaos, even if only on small sets in the phase space.[1] Thus the existence of a map with an invariant, (3), is a notable phenomenon. Notwithstanding their rarity, such maps provide valuable examples, especially as a starting point for perturbation theory. The existence of an invariant does not necessarily mean the map is globally integrable in the sense of Liouville–Arnold. In the latter case all of the invariant curves are homotopic—this rules out even the case of the pendulum since the invariant curves have two distinct topologies corresponding to oscillating and rotating motion, respectively. Globally integrable maps are conjugate to the Birkhoff normal form $f(J,\theta)=(J,\theta+\Omega(J))$.[2] More generally, the invariant will have level curves that are not homotopically equivalent. Birkhoff refers to this case as locally integrable.[3]

It is easy, in principle, to construct a locally integrable map on $\mathbb{R}^2$, since any symplectic map obtained from a one degree-of-freedom Hamiltonian flow has the energy as an invariant. However, explicit forms for such maps are not so easily obtained, except for those few cases where Hamilton's equations can be explicitly integrated. The first nontrivial example, apart from the pendulum, was the elliptical billiard;[3] however, the explicit form of this map is not easy to write down. A more explicit example is the rational family due to McMillan.[4] A generalization of this family was discovered by Refs. 5,6; however, these maps are not area-preserving except in the McMillan case, though they can be reversible.

A systematic procedure for constructing locally inte-

grable, area-preserving maps was devised by Suris.[7] He studied maps of the second difference form,

$$x_{t+1}-2x_t+x_{t-1}=\epsilon F(x_t,\epsilon), \tag{6}$$

which can be thought of as an area-preserving map upon defining the variables $(x,x')=(x_{t-1},x_t)$. Under the assumptions that F and Φ are analytic and the invariant has the form,

$$\Phi(x,x',\epsilon)=\Phi(x',x,\epsilon)=\phi_0(x,x')+\epsilon\phi_1(x,x'), \tag{7}$$

Suris showed there are exactly three possible families. For these cases the corresponding F is rational in x, in trigonometric functions of x, or in exponentials of x, respectively. The three examples of the form (1) that we construct in Sec. II correspond to these three cases; however unlike Suris we have not shown that our solutions are exhaustive.

Other examples of integrable symplectic maps have also been found. Suris' techniques have been used to find higher dimensional, integrable symplectic maps.[8,9] Another technique that gives many examples is to find appropriate discretizations of integrable differential equations; these can be treated with the methods obtained from inverse scattering theory.[10,11] Finally, maps with integrals have been constructed as integration algorithms for differential equations with conserved quantities.[12]

In this paper we will study volume-preserving maps on $\mathbb{R}^3$. Such maps are useful in understanding the motion of passive tracers in fluids[13] and magnetic field line configurations.[14,15] They are also of interest since many phenomena in the two-dimensional case are not yet completely understood in higher dimensions. Such phenomena include transport,[16,17] the breakup of heteroclinic connections,[18,19] and the existence of invariant tori.[20,21] These maps are also important as integrators for incompressible flows; in some cases the maps are constructed to be volume-preserving,[22–25] and in others to preserve the conserved quantities of the flow.[12]

A prominent class of volume-preserving maps that have an invariant are trace maps.[26] Physically, these are obtained from the Schrödinger equation with a quasiperiodic potential.[27] Mathematically, they arise from substitution rules on matrices.[26,28,29] As an example, consider matrices $A,B \in SL(2,\mathbb{R})$, the group of 2×2 matrices with unit determinant. A substitution rule acts on a string of matrices and corresponds to replacements of each occurrence of A and B with strings of these matrices. One of the most studied examples is the Fibonacci substitution rule which corresponds to $A\mapsto B$ and $B\mapsto AB$. The trace map is determined by the action of this substitution on the traces of the matrices. Defining $x=\frac{1}{2}\mathrm{Tr}(A)$, $y=\frac{1}{2}\mathrm{Tr}(B)$, and $z=\frac{1}{2}\mathrm{Tr}(AB)$, then the substitution rule gives $x'=\frac{1}{2}\mathrm{Tr}(B)=y$, $y'=\frac{1}{2}\mathrm{Tr}(AB)=z$, and $z'=\frac{1}{2}\mathrm{Tr}(BAB)=\frac{1}{2}\mathrm{Tr}(AB^2)=-x+2yz$, where we use the Cayley–Hamilton theorem to simplify the last equation. Thus we obtain the three-dimensional mapping,

$$f(x,y,z)=(y,z,-x+2yz). \tag{8}$$

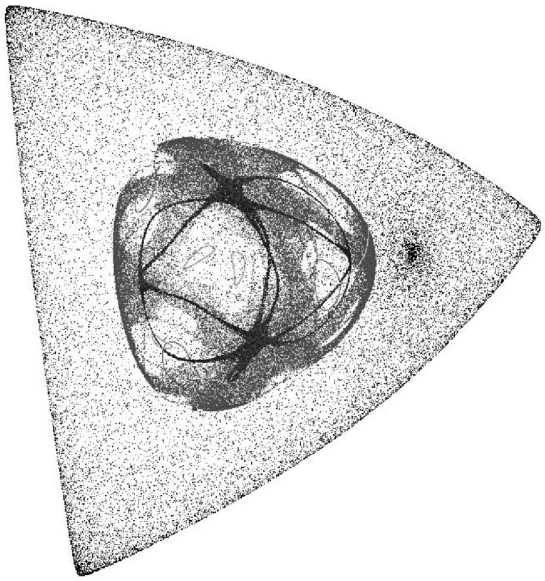

FIG. 1. Some orbits of the cubic trace map (10). The outermost orbit lies on the level $\mu=0$.

This map has a form similar to (1) and is volume-preserving, but the change in sign in the last term means the map is orientation-reversing. All trace maps that arise from invertible substitution rules have the function,

$$\Phi(x,y,z)=x^2+y^2+z^2-2xyz-1, \tag{9}$$

as an invariant. Roberts calls this function the Fricke–Vogt invariant;[28] it is an example of a group theoretic invariant called a character. In this case, (9) arises from the trace of the word $A^{-1}B^{-1}AB$. There are also orientation-preserving trace maps, though no nontrivial quadratic ones. A simple cubic example is

$$f(x,y,z)=(-y+2xz,z,-x-2yz+4xz^2). \tag{10}$$

While trace maps are polynomial maps that have an invariant, it is interesting to note that there are no nontrivial, polynomial, locally integrable maps in two dimensions.[2]

Maps, such as (8) and (10), that preserve the Fricke–Vogt invariant have orbits that are confined to the two-dimensional level sets, M_μ defined in (5), for (9). When μ is in the range $-1<\mu<0$, M_μ has a compact component that is topologically a sphere. Orbits on this sphere become increasingly chaotic as μ increases towards 0, see Fig. 1. At $\mu=0$, the compact component becomes a tetrahedron (a sphere with four corners) that is joined to the unbounded pieces at the four critical points of Φ. Orbits on the tetrahedron are still confined, and their dynamics is semiconjugate to the hyperbolic torus map $(\theta,\psi)\to(\psi,\theta+\psi)$.[26] Recall that a semiconjugacy is a many-to-one relationship between two dynamical systems, while a conjugacy is one-to-one; in this case the map is two-to-one.

The dynamics of the map (1)–(2) is at least as complex. We will see in Sec. III that the components of the level sets of (4) are topologically points, circles, spheres, tori or unbounded sets depending upon the values of the parameters and μ. We will use the critical points of (4), and their orbits to help classify these cases. We also find the low period

orbits and their bifurcations. The existence of the invariant implies that these orbits come in one parameter families that are transverse to the level sets M_μ, except at bifurcation points. We will also show some numerical examples of the dynamics.

One reason for studying maps of the form (1) is that they are volume-preserving for arbitrary F. Moreover, this form also arises quite generally for the case of quadratic automorphisms. According to Ref. 30, any such map that is nontrivial, volume and orientation-preserving is conjugate to the normal form (1), where F is replaced by

$$Q(y,z)=\alpha+\tau z-\sigma y+ay^2+byz+cz^2, \tag{11}$$

a quadratic polynomial.

II. CONSTRUCTION OF THE INVARIANT

Motivated by the fact that quadratic case has the normal form (1), we will use the techniques of Suris to construct maps of this form that have an invariant. It is convenient to introduce a parameter ϵ by scaling the variables $(x,y,z)\to\epsilon(x,y,z)$, and defining a new function $2F(y,z,\epsilon)=\epsilon^{-2}F(\epsilon y,\epsilon z)$ so that (1) becomes

$$f_\epsilon(x,y,z)=(y,z,x+2\epsilon F(y,z,\epsilon)). \tag{12}$$

The factor of 2 is added to simplify some of the intermediate results. In the case of quadratic maps, since $Q(\epsilon y,\epsilon z)=\epsilon^2 Q(y,z)$, the nonlinear function in the scaled coordinates does not involve ϵ; however in the general case it does, so we allow for this dependence. We will assume that $F(y,z,\epsilon)$ depends smoothly on ϵ.

It is convenient to write (12) as a third difference equation, by noting that

$$f_\epsilon(x_{n-1},x_n,x_{n+1})=(x_n,x_{n+1},x_{n+2}),$$

where x_{n+2} is given by

$$x_{n+2}=x_{n-1}+2\epsilon F(x_n,x_{n+1},\epsilon).$$

The map is now in a form analogous to that studied by Suris (6). If Φ_ϵ is an invariant for f_ϵ, then for all n,

$$\Phi_\epsilon(x_{n-1},x_n,x_{n+1})=\Phi_\epsilon(x_n,x_{n+1},x_{n+2}), \tag{13}$$

which in terms of x, y, and z leads to

$$\Phi_\epsilon(x,y,z)=\Phi_\epsilon(y,z,x+2\epsilon F(y,z,\epsilon)). \tag{14}$$

Since $-x_{n-1}=-x_{n+2}+2\epsilon F(x_n,x_{n+1},\epsilon)$, it follows that Φ_ϵ should also satisfy

$$\Phi_\epsilon(-x_{n+2},x_n,x_{n+1})=\Phi_\epsilon(x_n,x_{n+1},-x_{n-1})$$

which suggests considering invariants satisfying the symmetry ansatz

$$\Phi_\epsilon(x,y,z)=\Phi_\epsilon(y,z,-x). \tag{15}$$

In fact, following (7) our attention will be focussed on invariants of the form,

$$\Phi_\epsilon(x,y,z)=\phi_0(x,y,z)+\epsilon\phi_1(x,y,z), \tag{16}$$

satisfying condition (15). With these assumptions we can obtain the following proposition.

Proposition 1: *Let $F(y,z,\epsilon)$ be a smooth function defined on some neighborhood of $\epsilon=0$. Suppose that for $|\epsilon|<\epsilon_0$ there exist smooth, real valued functions ϕ_0 and ϕ_1 such that Φ_ϵ defined by* (16) *satisfies* (14) *and* (15). *Then ϕ_0 is even, invariant respect to cyclic permutations of the variables and satisfies*

$$\partial_\xi\left(\frac{\partial_{\xi\xi\xi}\phi_0}{\partial_\xi\phi_0}\right)=0,\ \xi=x,y,z. \tag{17}$$

Proof: Setting $u_n=\epsilon F(x_n,x_{n+1},\epsilon)+x_{n-1}$, we have $x_{n+2}=\epsilon F(x_n,x_{n+1},\epsilon)+u_n$ and $x_{n-1}=-\epsilon F(x_n,x_{n+1},\epsilon)+u_n$. In that case (13) and (15) imply

$$\Phi_\epsilon(x_n,x_{n+1},\epsilon F(x_n,x_{n+1},\epsilon)-u_n)=\Phi_\epsilon(x_n,x_{n+1},\epsilon F(x_n,x_{n+1},\epsilon)+u_n). \tag{18}$$

As $\phi_0=\Phi_0$ we have $\phi_0(x,y,-u)=\phi_0(x,y,u)$ and $\phi_0(x,y,u)=\phi_0(y,u,x)$. Therefore ϕ_0 is even and invariant respect to any cyclic permutation of the variables. Now, after renaming $x=x_n$, $y=x_{n+1}$ and $u=u_n$, we differentiate (18) three times with respect to ϵ and set $\epsilon=0$ to obtain

$$2\partial_z\phi_0(x,y,u)F|_0=\phi_1(x,y,-u)-\phi_1(x,y,u), \tag{19}$$

$$2\partial_z\phi_0(x,y,u)\partial_\epsilon F|_0=(\partial_z\phi_1(x,y,-u)-\partial_z\phi_1(x,y,u))F|_0, \tag{20}$$

and

$$\begin{aligned}2\partial_{zzz}\phi_0(x,y,u)(F|_0)^3+6\partial_z\phi_0(x,y,u)\partial_{\epsilon\epsilon}F|_0&=3(\partial_{zz}\phi_1(x,y,-u)-\partial_{zz}\phi_1(x,y,u))(F|_0)^2\\&\quad+6(\partial_z\phi_1(x,y,-u)-\partial_z\phi_1(x,y,u))\partial_\epsilon F|_0,\end{aligned} \tag{21}$$

where $F|_0$, $\partial_\epsilon F|_0$, and $\partial_{\epsilon\epsilon}F|_0$ stand for F and its partial derivatives evaluated at $(x,y,0)$. Differentiating (19) twice w.r.t. u and using (20) and (21) yields

$$-4\partial_{zzz}\phi_0(x,y,u)(F|_0)^3+6\partial_z\phi_0(x,y,u)\left(\partial_{\epsilon\epsilon}F|_0-2\frac{(\partial_\epsilon F|_0)^2}{F|_0}\right)=0. \tag{22}$$

Since $F|_0$ is independent of u, the result then follows for $\xi=z$. The proof is completed upon noting that ϕ_0 is invariant respect to cyclic permutations of the variables. □

A. Rational case

Note that if we assume that F does not depend on ϵ, then (22) as an equation for ϕ_0, reduces to

$$\partial_{\xi\xi\xi}\phi_0=0,\ \xi=x,y,z.$$

Indeed this would be the case if, e.g., we were to consider the family obtained from rescaling the homogeneous quadratic case, (11) with $\alpha=\tau=\sigma=0$. As this is also a particular solution of (17), this may also yield solutions for more general F as well. We now explore precisely those ϕ_0 satisfying that

condition. In such cases, ϕ_0 is a polynomial of degree at most two in each variable. Since ϕ_0 is even and invariant under cyclic permutation, we have

$$\phi_0(x,y,z)=a_0(x^2+y^2+z^2) + b_0(x^2y^2+y^2z^2+z^2x^2)+c_0\,x^2y^2z^2, \quad (23)$$

up to additive constants. From (20) it follows that

$$(\phi_1(x,y,u)+\phi_1(x,y,-u))F|_0 = -2\,\phi_0(x,y,u)\partial_\epsilon F|_0+k(x,y),$$

where $k(x,y)$ is some function not depending on u. Taking into account (19) gives

$$2\,\phi_1(x,y,u)F|_0=-2\,\partial_z\phi_0(x,y,u)(F|_0)^2 - 2\,\phi_0(x,y,u)\partial_\epsilon F|_0+k(x,y),$$

therefore ϕ_1 is a polynomial of degree at most 2 in u and by the symmetry condition (15) we obtain

$$\phi_1(x,y,z)=a(x^2+y^2+z^2)+b(x^2y^2+y^2z^2+z^2x^2) + c\,x^2y^2z^2+d(xy+yz-zx) + e(x^2yz+z^2xy-y^2zx). \quad (24)$$

Finally, upon using (23) and (24) in Eq. (18), and solving for F yields

$$2\,F(y,z,\epsilon) = \frac{(y-z)(d-e\,yz)}{a_0+\epsilon a+(b_0+\epsilon b)(y^2+z^2)+(c_0+\epsilon c)y^2\,z^2+\epsilon e\,y\,z}.$$

Notice that F is a polynomial only when $e=0$, thus the only polynomial case is linear, and therefore dynamically trivial.

Many of the parameters in F are superfluous. As we are interested in maps that do not have singularities, we can assume that the origin is not a singular point. Then $a_0+\epsilon a \neq 0$, and we can rewrite the above equation so that there are only four essential parameters, and the map becomes (1) with F given by (2), and invariant given by (4). Moreover, after rescaling we are reduced to three, 3-parameter families corresponding to $\delta=0,\pm 1$.

B. Other solutions

While we have not investigated all solutions of (17), it is possible to find other explicit solutions if we assume that the first integral of this equation is given by

$$\frac{\partial_{\xi\xi\xi}\phi_0}{\partial_\xi\phi_0}=\text{const},\ \xi=x,\,y,\,z; \quad (25)$$

thus, we assume that the right-hand side is constant instead of being a function of the remaining two variables. There are two possible forms, depending upon the sign of the constant. When $\text{const}=-\omega^2\neq 0$ we obtain a solution that contains trigonometric functions. Eliminating unnecessary parameters we obtain a family of maps of the form (1) with

$$F(y,z)=2\,\arctan\left(\frac{\alpha(\sin z-\sin y)+\beta\sin(z-y)}{\chi+\gamma(\cos y+\cos z)+\beta\sin y\sin z+\delta\cos y\cos z}\right).$$

This family has invariants given by

$$\Phi(x,y,z)=\chi(\cos x+\cos y+\cos z)+\alpha(\sin x\sin y+\sin y\sin z-\sin z\sin x)+\beta(\sin x\sin\, y\cos z+\sin y\sin z\cos x - \sin z\sin x\cos y)+\gamma(\cos x\cos y+\cos y\cos z+\cos z\cos x)+\delta\cos x\cos y\cos z. \quad (26)$$

The case when the constant is positive, $\text{const}=\omega^2\neq 0$, produces a similar family of maps but replaces the trigonometric functions with hyperbolic ones. Thus F becomes

$$F(y,z)=2\,\text{arctanh}\left(\frac{\alpha(\sinh y-\sinh z)+\beta\sinh(y-z)}{\chi+\gamma(\cosh y+\cosh z)+\beta\sinh y\sinh z+\delta\cosh y\cosh z}\right),$$

and the invariants are given by (26) with sin and cos replaced by the corresponding hyperbolic functions. In both of these cases some restrictions on parameters would be necessary to avoid singularities.

However unlike Ref. 7, our results do not exclude the existence of additional families of maps having invariants of the type considered in Proposition 1. For example, the most general first integral of (17) involves arbitrary functions whose signs could change depending upon position, thus causing a switch from trigonometric to hyperbolic behavior. Certainly there exist solutions of (17) that are even and cyclic permutation invariant but which do not satisfy (25), as, for example, $\phi_0(x,y,z)=\cos xyz$ and $\phi_0=\cosh xyz$. These two particular solutions also give rise to families of maps with an invariant Φ, however these maps have singular points.

Finally we investigate the orientation reversing analog of (1),

$$(x,y,z)\to(y,z,-x+F(y,z)). \quad (27)$$

Introducing the parameter ϵ as before, means that we wish to find solutions to

$$\Phi_\epsilon(x,y,z)=\Phi_\epsilon(y,z,-x+2\epsilon F(y,z,\epsilon)).$$

Then the symmetry ansatz, (15), should be replaced by

$$\Phi_\epsilon(x,y,z)=\Phi_\epsilon(y,z,x).$$

These conditions lead to the same result as before, namely, Eq. (17) in Proposition 1. If, as before, we consider the simplest case $\partial_{zzz}\phi_0=0$, we still obtain ϕ_0 of the form (23).

The result for (27), after assuming the origin is not a singular point and scaling out inessential constants becomes

$$F(y,z)=-\frac{\alpha+(\beta+\gamma yz)(y+z)+\delta y^2+\chi yz+\eta z^2+\kappa y^2z^2}{1+\eta y+\delta z+\gamma yz+\lambda(y^2+z^2)+\kappa yz(y+z)+\mu y^2z^2}. \tag{28}$$

This map has the invariant,

$$\Phi(x,y,z)=x^2+y^2+z^2+(\alpha+\gamma xyz)(x+y+z)+(\beta+\kappa xyz)(xy+yz+zx)+\eta(x^2y+y^2z+z^2x)+\delta(xy^2+yz^2+zx^2)$$
$$+\chi xyz+\lambda(x^2y^2+y^2z^2+z^2x^2)+\mu x^2y^2z^2. \tag{29}$$

Note that the Fibonacci map (8) can be recovered from this result by setting $\chi=-2$ and all of the other parameters to zero. A slightly more general polynomial map can also be obtained by letting α and β be nonzero, which gives

$$(x,y,z)\to(y,z,-x-\alpha-\beta(y+z)-2yz).$$

This map is not conjugate to the Fibonacci map, as the level sets of Φ are topologically different from those of (9).

III. DYNAMICS

In this section we will study the dynamics of the rational map f given by (1)–(2). We begin with a brief discussion of some general properties of volume-preserving maps, then consider properties specific to f.

Recall that this map has three free parameters, α,β,γ and one index $\delta=0,\pm1$. The map is defined on all of $\mathbb{R}^3$ if and only if

$$\delta=1,\quad \gamma\geqslant 0\quad\text{and}\quad |\beta|<2(\gamma+1)$$
$$\text{or}$$
$$\delta=0,\quad \gamma>0\quad\text{and}\quad |\beta|\leqslant 2\gamma. \tag{30}$$

In these cases f is a diffeomorphism. Only parameters satisfying such conditions will be considered in this section.

A. Volume-preserving maps with an invariant

In this section we will discuss some general properties of volume preserving maps with an invariant. As is well known,[26,28] the dynamics of these maps restricted to a noncritical level set M_μ, (5), is equivalent to those of a measure preserving map. Moreover, the existence of the invariant implies that orbits typically come in one-parameter families.

Lemma 2: *Let f be a volume-preserving diffeomorphism on* $\mathbb{R}^d$ *with a smooth invariant* Φ.

Suppose that ξ_0 *is a noncritical point of* Φ *that is periodic of period n for f. Then* f^n *is locally equivalent to a parametrized family of* $d-1$ *dimensional maps. The linear map* $Df^n(\xi_0)^T$ *has an eigenvector* $\nabla\Phi(\xi_0)$, *whose multiplier is 1 and the remaining multipliers correspond to the restriction of* f^n *to* $\Phi(\xi_0)=\mu_0$. *Moreover, if* 1 *is a multiplier of multiplicity one, then there is a unique curve,* $\xi(\mu)$ *of period n orbits through* ξ_0.

On the other hand if ξ_0 *is a critical point of* Φ, *so are all points in the orbit of* ξ_0.

Proof: Since $\Phi(f(\xi))=\Phi(\xi)$ for any ξ, we can differentiate to obtain $D\Phi(f(\xi))\circ Df(\xi)=D\Phi(\xi)$, or in terms of the gradient,

$$Df(\xi)^T\nabla\Phi(f(\xi))=\nabla\Phi(\xi).$$

Thus since Df is nondegenerate, whenever ξ_0 is a critical point so is its image. This proves the last assertion. When ξ_0 is a period-n orbit, this relation applied to f^n implies

$$(Df^n(\xi_0))^T\nabla\Phi(\xi_0)=\nabla\Phi(\xi_0),$$

which implies that $\nabla\Phi(\xi_0)$ is an eigenvector with multiplier 1, as promised.

When ξ_0 is not a critical point, the set M_μ is a smooth submanifold at ξ_0. Thus, according to the inverse function theorem there exists a linear projection $\pi(\xi)=\zeta\in\mathbb{R}^{d-1}$ such that the map $h(\xi)=(\pi(\xi),\Phi(\xi))$ is a diffeomorphism on a neighborhood of ξ_0. Locally, the map $h\circ f^n\circ h^{-1}(\zeta,\mu)=(\zeta',\mu)$ is well defined and has 1 as a multiplier associated to the parameter μ, so the remaining multipliers are associated with the map $\zeta\to\zeta'$. Finally, let $G:\mathbb{R}^d\times\mathbb{R}\to\mathbb{R}^d$ be given by $G(\xi,\mu)=(\pi(f^n(\xi)-\xi),\Phi(\xi)-\mu)$. It is easy to see that the Jacobian

$$D_\xi G(\xi_0,\mu_0)=\begin{pmatrix}\pi(Df^n(\xi_0)-I)\\ D\Phi(\xi_0)\end{pmatrix}$$

has rank d. Since we know the solution $G(\xi_0,\mu_0)=0$, the implicit function theorem implies that there exists a unique solution, ξ_μ, to $G=0$ in a neighborhood of μ_0. □

When $d=3$, the characteristic polynomial for the multipliers has the form $p(\lambda)=\lambda^3-t\lambda^2+s\lambda-1$, where $t=\mathrm{Tr}(Df^n)$, and $s=\frac{1}{2}[t^2-\mathrm{Tr}((Df^n)^2)]$. Therefore, when $\lambda=1$ is a multiplier, $s=t$ and the characteristic equation reduces to

$$\lambda^3-t\lambda^2+t\lambda-1=(\lambda-1)(\lambda^2-(t-1)\lambda+1)=0,$$

so that the remaining multipliers satisfy $\lambda_1+\lambda_2=t-1$. These two multipliers correspond to the map restricted to the invariant surface when the orbit is not in the critical set of Φ. Thus if we consider the restricted map, the periodic orbit is elliptic if $-1<t<3$, hyperbolic with reflection if $t<-1$, and hyperbolic if $t>3$. If $t=-1$, the restricted map has a double multiplier at -1, so that a period-doubling is expected. In the case $t=3$, $\lambda=1$ is a double eigenvalue and a saddle-center bifurcation is expected. More generally suppose that ξ_0 is not a critical point of Φ and that at this point a curve of period n points, intersects a period $k\cdot n$ curve. Then the linearization of f^n at ξ_0 must have a k^{th} root of unity as eigenvalue so that $t=1+2\cos(2\pi(m/k))$ for some integer m.

B. Invariant surfaces

The topology of the level sets of the invariant (4),

$$\Phi(x,y,z)=x^2+y^2+z^2+\alpha(xy+yz-zx)+\gamma(x^2y^2+y^2z^2+z^2x^2)+\beta(x^2yz+z^2xy-y^2zx)+\delta x^2y^2z^2,$$

depends significantly on the parameters α, β, and γ, as well as the index δ. As we will see, the components of these sets can be points, circles, spheres, tori, or noncompact. For some parameter values all of the level sets are compact, while for others there are compact components for certain ranges of μ. Of course, when the parameters are fixed the topology of M_μ can change only at critical values of μ, i.e., on level sets containing critical points of Φ, so our first task is to find these.

The equations for the critical points, $\nabla\Phi=0$, reduce to

$$2x=-F(y,z),\ 2y=-F(z,-x),\ 2z=-F(-x,-y),$$

where F is given in (2) and we have assumed—as always in this section—that it is never singular. Thus, on critical points the map f acts as $(x,y,z)\to(y,z,-x)$. This implies that the critical orbits are at most period 6.

The fixed point at the origin is always a critical point. The origin is local minimum of Φ when $-2<\alpha<1$ so that the surfaces are locally spheres. It is a saddle when $\alpha<-2$ or $\alpha>1$, so that the surfaces are locally a family of hyperbolic cylinders.

To obtain more explicit expressions for the remaining critical points, note that the level surfaces have a discrete symmetry, corresponding to the transformation $(x,y,z)\to(y,z,-x)$, which is a $\pi/3$ rotation around $x=-y=z$ followed by a reflection through $x-y+z=0$. To make this more explicit, it is often convenient to introduce rotated coordinates so that the vertical axis coincides with $x=-y=z$. In particular we define cylindrical coordinates (r,θ,ζ), determined by

$$r\cos\theta=\frac{1}{\sqrt{2}}(x+y),\ r\sin\theta=\frac{1}{\sqrt{6}}(-x+y+2z),\qquad \zeta=\frac{1}{\sqrt{3}}(x-y+z). \tag{31}$$

In these coordinates (4) becomes

$$\Phi(r,\theta,\zeta)=\frac{\delta}{54}r^6(\sin 3\theta)^2+\frac{\sqrt{2}}{54}(9(\beta+2\gamma)+\delta(3r^2-2\zeta^2))r^3\zeta\sin 3\theta+\frac{1}{3}(\gamma-\beta)\zeta^4+\frac{1}{4}\gamma r^4+\frac{1}{2}\beta r^2\zeta^2+\left(1+\frac{\alpha}{2}\right)r^2+(1-\alpha)\zeta^2+\frac{\delta}{108}\zeta^2(2\zeta^2-3r^2)^2. \tag{32}$$

This is especially simple when $\delta=0$, and $\beta=-2\gamma$, because all of the θ-dependent terms vanish, and so the surfaces have cylindrical symmetry. We exploit this in some of the examples below.

The critical points of Φ can be computed explicitly in a rather general way using (32). There are five classes of critical points:

C0. The origin is always a fixed critical point.

C1. There are up to two critical orbits of period 2, which correspond to points $(x,-x,x)$ where x a real root of $\delta x^4+2(\gamma-\beta)x^2+1-\alpha=0$.

C2. There are up to three critical orbits of period 6, corresponding to points (x,y,x), where x and y are given by any real solutions of

$$0=2\delta\gamma x^6+(4\gamma^2-\beta^2+\delta(2-\alpha))x^4+6\gamma x^2+2+\alpha,\qquad y=-\frac{\beta x^3+\alpha x}{\delta x^4+(2\gamma-\beta)x^2+1}. \tag{33}$$

The orbits are generated by the period six symmetry of M_μ, so two points from these orbits lie on each of the three planes $x=z$, $z=-y$, and $y=-x$.

C3. If $\alpha<-2$ and $\gamma>0$ there exists an additional period 6 critical orbit, generated by $(x_0,x_0,0)$, where $x_0=\sqrt{-(2+\alpha)/2\gamma}$. Such orbits lie on the plane $y=x+z$.

C4. Finally in the special case $(2\gamma+\beta)=2\delta$ it is possible that there exist curves of critical orbits. When they exist, these curves include the orbits (**C2**) and (**C3**). The simplest case is $\delta=0$, when the surfaces have cylindrical symmetry. Then the circle of radius $\sqrt{-(2+\alpha)/\gamma}$ in the plane $y=x+z$ is critical providing $\alpha<-2$, $\gamma>0$. Every orbit on the critical circle is period 6, and the circle contains the critical orbit (**C3**). The case $\delta=1$ is more complex. In the coordinate system (31), the critical curves are given by

$$\zeta^2=\frac{2+\alpha+\gamma r^2}{2\gamma},\qquad \sin 3\theta=\zeta\frac{2+\alpha-2\gamma(9+r^2)}{\sqrt{2}\gamma r^3}. \tag{34}$$

Solutions only exist when $\alpha<-2$ or $\alpha>18\gamma-2$. When $\alpha<-2$, (34) represents one closed curve. For $\alpha>18\gamma-2$, (34) corresponds to two closed curves lying on each side of $y=x+z$.

For the special case $\delta=0$, we can relatively easily classify the possible topologies of the sets M_μ. In this case there is at most one critical orbit in each of the classes described above. We label the critical levels corresponding to the (**Ci**) by μ_i. When they exist, the critical levels appear in the order

$$\mu_2 \leqslant \mu_3=\mu_4 \leqslant \mu_0=0$$

while μ_1 may vary in the ordering.

When $\alpha<-2$ there are two period six orbits. The first, (**C2**), is born at μ_2 which has an expression—arising from the discriminant of (33)—that is too long to display. The second period six orbit (**C3**) is born at

$$\mu_3=-\frac{(2+\alpha)^2}{4\gamma}.$$

The critical circle (**C4**) exists when $\beta=-2\gamma$ and $\alpha<-2$. In this case $\mu_4=\mu_3=\mu_2$, and the orbits (**C2**) and (**C3**) become part of the critical curve. Finally the period two critical orbit arises only when $(1-\alpha)/(\gamma-\beta)<0$ at the level

$$\mu_1=\frac{3(\alpha-1)^2}{4(\beta-\gamma)}.$$

In the special case $\alpha=1, \gamma=\beta$ all points on the axis $(x, -x, x)$ are critical of period 2 and they lie on the level $\mu=\mu_1=\mu_0=0$.

To complete the classification of the foliation $\{M_\mu, \mu \in \mathbb{R}\}$ for $\delta=0$, we use (32) to describe cross sections on the $\zeta=$const planes, and take into account the critical points. Let $\mu_{\min}$ (respectively, $\mu_{\max}$) the minimum (respectively, the maximum) of the levels where critical orbits arise.

When $\gamma<\beta$ all level sets are nonempty and unbounded; however, there can be compact components for some ranges of μ. In fact M_μ is composed of two unbounded cones lying on each side of $y=x+z$ for $\mu<\mu_{\min}$ while for $\mu>\mu_{\max}$, the level sets are unbounded cylinders surrounding the axis $x=-y=z$.

On the other hand if $\gamma>\beta$ the level sets are empty for $\mu<\mu_{\min}$ and homeomorphic to spheres if $\mu>\mu_{\max}$. In the range $\mu_{\min}<\mu<\mu_{\max}$ each M_μ is composed of one or more closed surfaces.

Taking into account the possible transitions we find the following families of level sets (see the illustrations in Fig. 2):

(1) $\gamma \geqslant \beta$, $\alpha<-2$: $M_\mu=\varnothing$ when $\mu<\mu_2$. For $\mu_2<\mu<\mu_3$, M_μ consists of six bubbles that develop from the critical orbit (**C2**). At $\mu=\mu_3$ these six components become connected at the (**C3**) orbit, creating a torus. At $\mu_0=0$, the torus changes into a sphere pinched at the origin when the (**C0**) point appears. The case $\beta=-2\gamma$ is special since $\mu_2=\mu_3$ and the torus develops directly from the critical circle (**C4**).

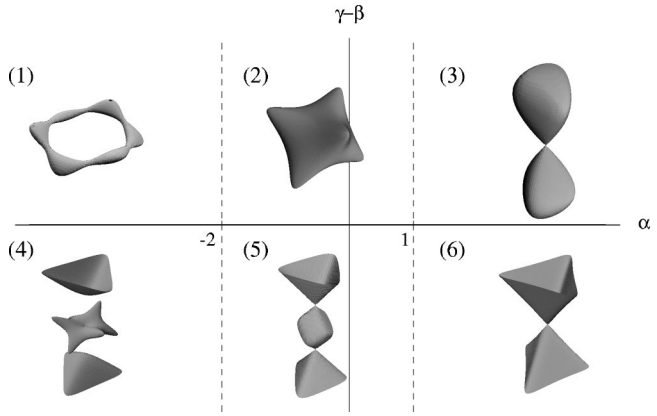

FIG. 2. Level sets of (32) for $\delta=0$. There are seven categories according to the parameter values of α and $\gamma-\beta$. Some of the most distinctive level sets in six of these families are displayed.

(2) $\gamma \geqslant \beta$, $-2 \leqslant \alpha \leqslant 1$, excluding the case $\alpha=1$, $\gamma=\beta$: The only critical point is the origin that arises at $\mu_0=0$. Subsequent level sets are homeomorphic to spheres that enclose the critical point.

(3) $\gamma>\beta$, $\alpha>1$: At $\mu=\mu_1$ the period two (**C1**) orbit appears, giving rise to two spherical components. At $\mu_0=0$ these components become attached by the critical point (**C0**).

(4) $\gamma<\beta$, $\alpha<-2$: In addition to unbounded cones, compact components develops as in case 1. However at $\mu=\mu_1$ the spherical component becomes attached to the unbounded cones by the (**C1**) orbit originating the unbounded cylinder.

(5) $\gamma<\beta$, $-2 \leqslant \alpha \leqslant 1$: A sphere develops from the critical point (**C0**). This set becomes joined to the unbounded cones by the (**C1**) orbit when $\mu=\mu_1$.

(6) $\gamma \leqslant \beta$, $\alpha>1$: No bounded components exist. The unbounded cones meet at the (**C0**) point when $\mu_0=0$ and become an unbounded cylinder.

(7) $\gamma=\beta$, $\alpha=1$: In this special case the level sets are empty for $\mu<\mu_0=0$. M_0 is the critical axis $x=-y=z$. This critical set gives rise to unbounded cylinders for positive μ.

C. Periodic orbits

In this subsection we describe the low period orbits of the map (1)–(2) and their bifurcations.

Every point on the diagonal $x=y=z$ is a fixed point. Fixed points on M_μ correspond to solutions of the equation,

$$\delta x^6+(3\gamma+\beta)x^4+(3+\alpha)x^2=\mu,$$

so that if $\mu \neq 0$ the number of fixed points on any given surface is even; when $\delta=1$ there are up to 6, and when $\delta=0$ there are up to 4. The origin, which is a critical fixed point, lies on M_0; this corresponds to the collapse of two fixed points into the critical one.

The stability of fixed points is determined by

$$t=\mathrm{Tr}(Df)=\partial_2 F(x,x)=\frac{\beta x^2-\alpha}{1+(2\gamma+\beta)x^2+\delta x^4}. \qquad (35)$$

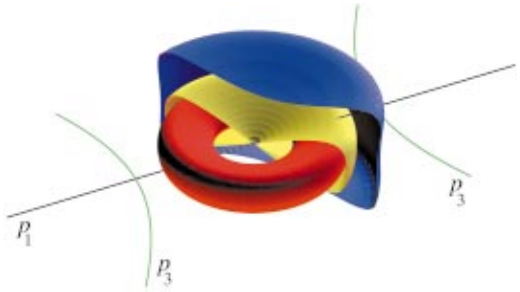

FIG. 3. (Color) Structure of level sets of Φ, (38), when $\alpha<-2$. Specifically, $\gamma=1$, $\alpha=-4$. Three level sets of Φ are shown: a torus for $\mu<0$, the critical pinched sphere at $\mu=0$ and a sphere for $\mu>0$. The line labeled p_1 is the line of fixed points, and the pair of curves labeled p_3 is one of three period three hyperbolas. The vertical axis corresponds to $x=-y=z$.

Even though the fixed point at the origin is critical, it always has one unit multiplier since it lies on the curve of fixed points. It is elliptic when $-3<\alpha<1$.

Period two points have the form $(x,y,x)\to(y,x,y)$, where x and y lie on the curve

$$\gamma(x^2+y^2)+2\beta xy+\delta x^2y^2=\alpha-1. \tag{36}$$

Using our standard assumptions (30), we see that this curve is an ellipse when $\delta=0$ if $\gamma>|\beta|$, and is otherwise a hyperbola. When $\delta=1$ the curve is bounded unless $\gamma=0$ and $\alpha\geqslant 1-\beta^2$.

The period two curves intersect the fixed point curves at the period doubling points, where the trace (35) is -1. This verifies that these points are period doubling bifurcations of the fixed points. The period two curves also intersect the critical orbits (**C1**) when they exist.

The stability of the period two orbits is determined by

$$\begin{aligned} t&=\partial_1F(x,y)+\partial_1F(y,x)+\partial_2F(x,y)\,\partial_2F(y,x)\\ &=3-4\frac{(x-y)^2(\gamma-\beta-\delta xy)}{\alpha-\beta xy}\\ &\quad-4\frac{(x-y)^2(\gamma x+\beta y+\delta xy^2)(\beta x+\gamma y+\delta x^2y)}{(\alpha-\beta xy)^2}, \end{aligned}$$

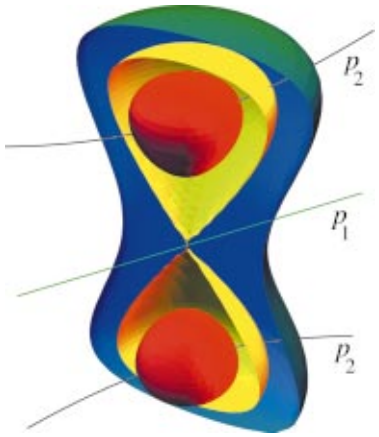

FIG. 4. (Color) Structure of the level sets M_μ for (38), when $\alpha>1$. Specifically, $\gamma=1$, $\alpha=2$. p_1, p_2 are the curves of points of period one and two, respectively. The vertical axis corresponds to $x=-y=z$.

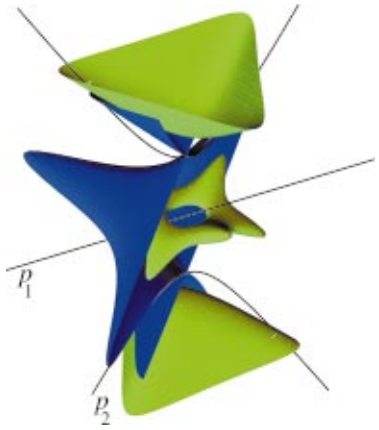

FIG. 5. (Color) Structure of the level sets M_μ for (32), with $(\alpha,\beta,\gamma,\delta)=(-4,2,1,0)$. The vertical axis corresponds to $x=-y=z$. Two level sets are shown, one for $\mu=-0.5$ contains a toroidal component, and a second for $\mu=18.75$ contains a spherical component.

where y and x satisfy (36).

For $\alpha,\beta\neq 0$ period three points lie on the hyperbolas, $(x,x,\alpha/\beta x)\to(x,\alpha/\beta x,x)\to(\alpha/\beta x,x,x)$. For a period 3 point (x,y,z) we have

$$\begin{aligned} t&=3+\partial_1F(y,z)\partial_2F(z,x)+\partial_1F(x,y)\partial_2F(y,z)\\ &\quad+\partial_1F(z,x)\partial_2F(x,y)+\partial_2F(x,y)\partial_2F(y,z)\partial_2F(z,x). \end{aligned} \tag{37}$$

The explicit expression for this is too long to display.

The fixed points undergo a tripling bifurcation when $t=0$, or equivalently when $x^2=\alpha/\beta$. This is exactly when the period three orbits collide with the fixed point line.

Next we illustrate the above discussion with some specific examples.

D. Examples

Example 3.1: In the particular case $\delta=0$, $\beta=-2\gamma$, Eq. (32) reduces to

$$\Phi(r,\theta,\zeta)=\frac{\gamma}{4}(r^2-2\zeta^2)^2+\left(1+\frac{\alpha}{2}\right)r^2+(1-\alpha)\zeta^2, \tag{38}$$

so that intersections of the level sets with planes perpendicular to the ζ axis are either circles or empty sets and the topology of M_μ as μ changes is especially easy to understand. In particular each M_μ is a closed surface so that f generates a bounded dynamics. When $\mu>\mu_{\max}$ the surface is topologically a sphere; for large μ has an hourglass shape that corresponds approximately to the dominant hyperbolic cylinder, $r^2-2\zeta^2=\text{const}$, determined by the first term in (38).

When $\alpha\leqslant -2$, the topology corresponds to case 1. The critical levels are:

(**C4**) $\mu_4=-(2+\alpha)^2/4\gamma$, corresponding to a critical circle of period six orbits in the plane $y=x+z$.

(**C0**) $\mu_0=0$, corresponding to the critical point at the origin. This case is illustrated in Fig. 3.

The case $\alpha>1$, whose topology corresponds to case 3, is illustrated in Fig. 4. In this case the critical levels are:

(**C1**) $\mu_1=-(\alpha-1)^2/4\gamma$, corresponding to the critical period two orbit.
(**C0**) $\mu_0=0$ corresponding to the critical point at the origin.

The fixed points lie on the line (x,x,x). If $\alpha<-3$ there are no fixed points on M_μ until $\mu=-[(3+\alpha)^2/4\gamma]$, when the line is tangent to the invariant surface at two points. As μ increases each of these splits into a pair of fixed points, one hyperbolic and the other elliptic; thus, each level set now contains four fixed points. When μ approaches 0 the two hyperbolic fixed points move to the origin, collapsing onto the critical fixed point at $\mu=0$. The remaining elliptic points period double at

$$\mu=\frac{(1-\alpha)(7+\alpha)}{4\gamma} \tag{39}$$

when the fixed point line meets the period two curve.

For $-3\leqslant\alpha\leqslant 1$ the fixed points line does not intersect M_μ for negative μ. For positive μ two elliptic fixed points appear on each M_μ. These points period double at (39) when the line crosses the period two curve.

When $\alpha>1$ fixed points also first appear on the invariant surfaces at $\mu=0$. Each of the fixed points is hyperbolic and remain so for all $\mu>0$.

Period two orbits (x,y,x) lie on the curve (36), which in this case is the hyperbola, $x=z$, $\gamma(x^2+y^2-4xy)=\alpha-1$. If $\alpha<1$ this hyperbola is tangent to M_μ when the fixed points period double, (39). This is a supercritical bifurcation, giving rise to a pair of elliptic period two orbits, and they later become hyperbolic when they period double as well.

The scenario is modified when $\alpha>1$, since the period two orbits are not born in a period doubling bifurcation. Instead they begin at the critical points (**C1**), when $\mu=-(\alpha-1)^2/4\gamma$. As μ increases, there are two period two orbits on each level set. When $\alpha\neq 4$ these orbits are initially elliptic, becoming hyperbolic after a period doubling. For $\alpha=4$ they are always hyperbolic with reflection.

Orbits of period three are generated by the intersection of the hyperbola $(x,x,\alpha/\beta x)$ with M_μ. Using (37), we find these orbits have $t=3$ at the solutions of

$$(2\gamma x^2+\alpha)^2(8\gamma^3x^6+4\gamma^2(2+\alpha)x^4-\alpha^2)=0.$$

The second factor in the equation above corresponds to a saddle-center bifurcation that creates two pairs of period three orbits on each level surface. As μ moves away from this bifurcation one of the orbits of each pair is hyperbolic and the other elliptic. When $\alpha>0$ there are no further bifurcations. The first factor above corresponds to the collision of the hyperbolic period three orbits with the fixed points. This only occurs when $\alpha<0$, on the surface $\mu=-[\alpha(\alpha+6)/4\gamma]$. The hyperbolic orbits pass through the fixed points, emerging again as hyperbolic—this corresponds to the standard scenario for tripling bifurcations in area-preserving mappings.[31]

The period three orbits undergo a period doubling when

$$2\gamma x^2+\alpha+2=0.$$

Thus if $\alpha\geqslant -2$ there is no period doubling, but the trace asymptotes to -1 as the orbit moves to infinity. When $\alpha<-2$ the elliptic orbits period double on the surface $\mu=-((2+\alpha)^3+2\alpha^2)/4\gamma(2+\alpha)$.

Example 3.2: For the general case, computations are not so simple. As an additional example we consider the case $(\alpha,\beta,\gamma,\delta)=(-4,2,1,0)$; this corresponds to the topology in case (4), see Fig. 5. For these parameter values the critical levels are:
(**C2**) $\mu_2=-\frac{43}{27}$, corresponding to a single period six orbit generated by $1/\sqrt{3}(1,\frac{10}{3},1)$.
(**C3**) $\mu_3=-1$, corresponding to a period six orbit generated by $(1,1,0)$.
(**C0**) $\mu_0=0$, corresponding to the critical point at the origin.
(**C1**) $\mu_1=18.75$, corresponding to a period two orbit at $x=-y=z=\pm\sqrt{\frac{5}{2}}$.

The evolution of fixed points is similar to the case $\alpha<-3$ of Example 3.1. The fixed point line is tangent to the invariant surface for $\mu=-\frac{1}{20}$ and then intersects M_μ at four points. The two orbits closer to the origin are hyperbolic while the other two are elliptic. The hyperbolic fixed points disappear as they collapse into the origin at $\mu=0$. However unlike Example 3.1 there is no period doubling and the remaining fixed points remain elliptic on all subsequent M_μ.

There are up to four period two orbits at the intersection of the level sets M_μ with the branches of the hyperbola (x,y,x), $x^2+y^2+4xy=-5$. When $\mu<-3.95501,...$ there is a pair of hyperbolic period two orbits on the unbounded components of M_μ. At this level a period doubling occurs, and the orbits become elliptic. At $\mu=18.75$ a pair of hyperbolic period two orbits emerge from the critical period two orbit (**C1**). At $\mu=31$ the hyperbola is tangent to M_μ, and the hyperbolic and elliptic orbits disappear in a saddle-center bifurcation.

Orbits of period three correspond to points on the hyperbola $(x,x,-2/x)$. Four period three orbits are born at $\mu\approx 17.8429$ in two simultaneous saddle-center bifurcations. The two hyperbolic orbits remain hyperbolic for larger μ, but the elliptic orbits undergo two period doubling bifurcations, becoming hyperbolic at $\mu\approx 17.9167$, and then elliptic again when $\mu\approx 27.4444$.

E. Numerical examples

In this section we present some numerical investigations of the dynamics of (1)–(2).

In Fig. 6 we show initial conditions on three level sets, for the same parameters as Fig. 3. The left panel shows the case $\mu=-0.69$, where the level set is a torus. In addition to several invariant circles with nontrivial homology, one can also see a chain of islands around an elliptic period five orbit (the blue orbit). For this μ, the fixed points do not yet exist. In the middle panel of Fig. 6, the critical level $\mu=0$ is shown. The origin, where the spherical surface is pinched, appears to be in the middle of a widespread chaotic zone. The domains covered by the orbits points near the origin with $\zeta>0$ (black points) and those with $\zeta<0$ (red points) are distinct. Away from the origin they are separated by a family of invariant circles, two of which are shown in the figure.

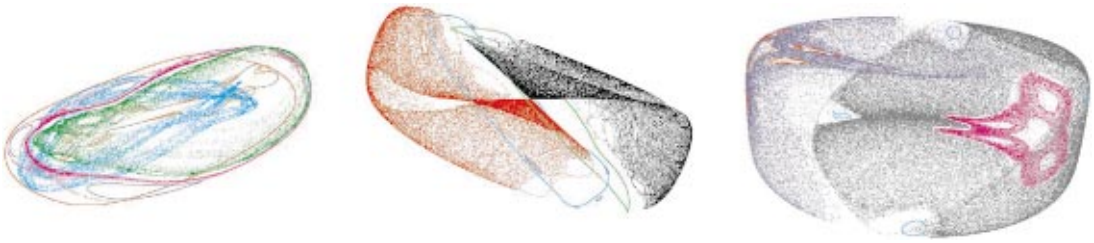

FIG. 6. (Color) Orbits of (1)–(2) for parameters $(\alpha,\beta,\gamma,\delta)=(-4,-2,1,0)$. Here some orbits on three level sets, $\mu=-0.69$, 0, and 1.0 are shown.

The right panel shows the dynamics for $\mu=1.0$. Here one can see a prominent island (purple) enclosing one of the elliptic fixed points. Again the invariant surface is divided into two large chaotic domains. For $\mu>1.1$ the large invariant circles have been destroyed, and the two chaotic zones are joined. There are prominent elliptic regions until after the fixed point orbit period doubles [from (39), $\mu=3.75$]. For larger μ the dynamics appears nearly uniformly chaotic; however, amongst the chaotic orbits are the islands surrounding the two elliptic period three orbits. These become more visible for large μ.

The orbits for the case corresponding to Fig. 4 are shown in Fig. 7. When $\frac{1}{4}<\mu<0$, the orbits that lie on the pair of spheres enclosing the critical period two orbit are predominantly regular, as can be seen in the left panel. As μ approaches 0, the chaotic regions grow, and they dominate the critical surface, $\mu=0$, as seen in the middle panel. There are also large islands surrounding the elliptic period two orbits at this level. Near $\mu=0.42$ a family of invariant circles appears that divides the chaotic region into two parts, as can be seen in the right panel. These circles are destroyed by $\mu=1.8$, and as before, apart from the elliptic period three orbits, the dynamics is largely chaotic as μ becomes large and the invariant surface acquires its hourglass shape.

As a final example, we consider the parameters corresponding to Fig. 5. For this case, orbits on compact components of six level sets are shown in Fig. 8. In the top-left panel, $\mu<-1$, and the orbits lie on a family of six spheres enclosing the (**C2**) orbit. In the next panel, these spheres have joined at the (**C3**) orbit, and the dynamics appears uniformly chaotic. In the top-right panel, $\mu=0$, the torus pinches at the origin. The red and black orbits encircle the elliptic fixed points. Also shown are green and yellow orbits that are associated with two elliptic period five orbits. For larger μ, as shown across the bottom row in Fig. 8, the islands around the elliptic fixed points remain prominent. Also visible are two elliptic period four orbits (light blue and green) in the bottom-middle panel at $\mu=5$. Apart from these islands, which persist on the unbounded components for $\mu>18.75$, the dynamics on these sets appears to be largely unbounded.

IV. CONCLUSIONS

We have used the methods of Suris to find several families of volume preserving maps on $\mathbb{R}^3$ that have an invariant. Unlike Suris, our solutions do not appear to be exhaustive. It would be interesting to obtain such a classification. We have not found any polynomial maps that have an invariant beyond the trace maps, (8)–(10). It may be that there are no polynomial, volume-preserving maps which have an invariant that satisfies the conditions (15)–(16); our results show this is true when F is a homogeneous quadratic function.

Both topologically and dynamically our maps are richer than the well-known trace maps. We do not know if there is a set of parameter values for which our maps are "completely chaotic" on an invariant surface; this was one of the prominent features of trace maps, which are semiconjugate to an Anosov system on the tetrahedral critical level set of the Fricke–Vogt invariant.

In the future it would be interesting to investigate the dynamics of these maps composed with a small perturbation that destroys the invariance of Φ. Is the transport between level sets more efficient when the dynamics on the surface is chaotic?

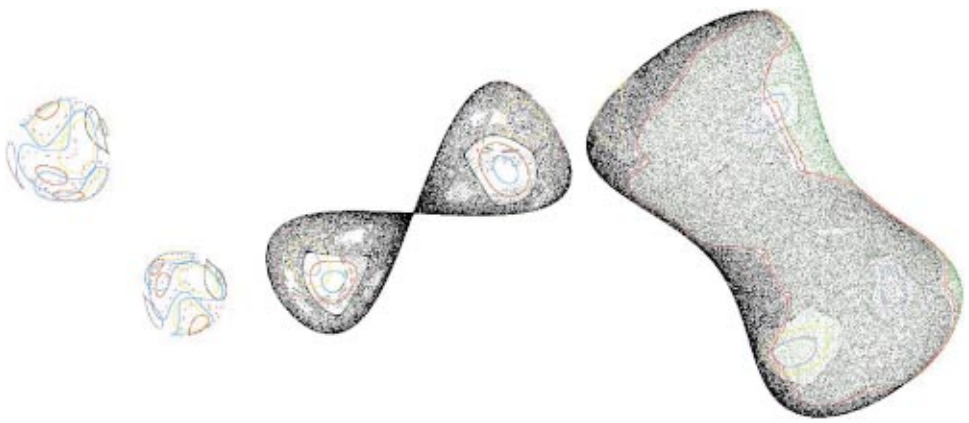

FIG. 7. (Color) Orbits of (1)–(2) for parameters $(\alpha,\beta,\gamma,\delta)=(2,-2,1,0)$. Here some orbits on three level sets, $\mu=-0.112$, 0, and 0.518 are shown.

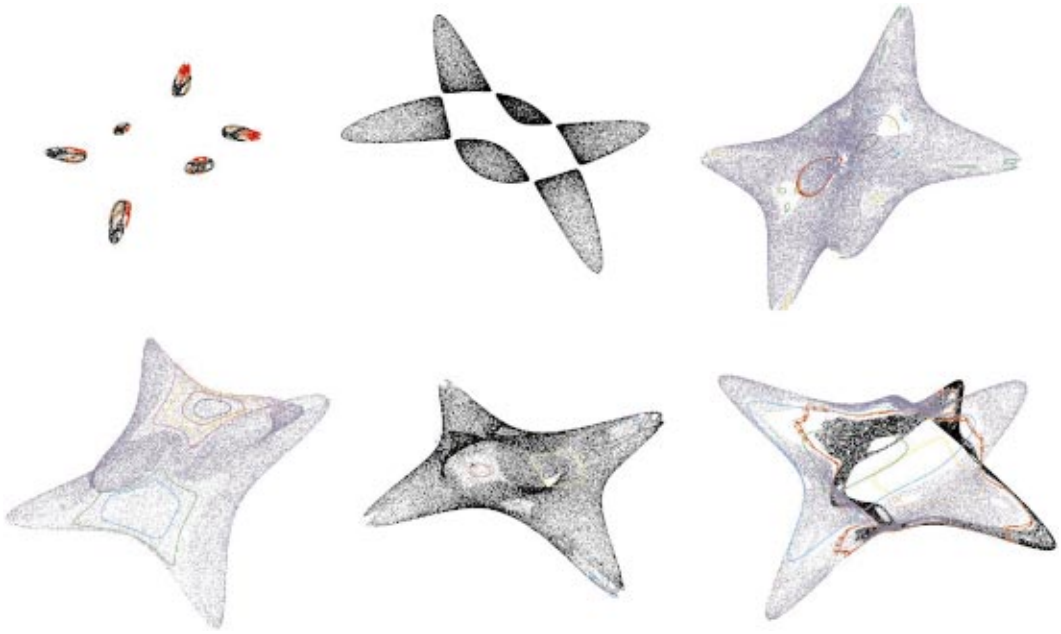

FIG. 8. (Color) Orbits of (1)–(2) for parameters $(\alpha,\beta,\gamma,\delta)=(-4,2,1,0)$. Across the top are shown orbits on the level sets $\mu=-1.4,-1.0,0.0$, and across the bottom are $\mu=1.0$, 5.0, and 17.6. The figures are not shown to the same scale.

ACKNOWLEDGMENTS

J.D.M. was supported in part by NSF Grant No. DMS-9971760, and the NSF VIGRE Grant No. DMS-9810751. A.G. was supported in part by the Thron Fellowship of the Department of Mathematics.

[1] J. D. Meiss, "Symplectic maps, variational principles, and transport," Rev. Mod. Phys. **64**, 795–848 (1992).
[2] A. P. Veselov, "Integrable mappings," Russ. Math. Surveys **46**, 1–51 (1991).
[3] G. D. Birkhoff, *Dynamical Systems*, Vol. 9 in *Colloquium Publications* (American Mathematical Society, New York, 1927).
[4] E. M. McMillan, "A problem in the stability of periodic systems," in *Topics in Modern Physics, a Tribute to E. V. Condon*, edited by E. E. Brittin and H. Odabasi (Colorado Assoc. Univ. Press, Boulder, 1971), pp. 219–244.
[5] G. R. W. Quispel, J. A. G. Roberts, and C. J. Thompson, "Integrable mappings and soliton equations," Phys. Lett. A **126**, 419–421 (1988).
[6] G. R. W. Quispel, J. A. G. Roberts, and C. J. Thompson, "Integrable mappings and soliton equations II," Physica D **34**, 183–192 (1989).
[7] Yu. B. Suris, "Integrable mappings of the standard type," Funct. Anal. Appl. **23**, 74–76 (1989).
[8] R. I. McLachlan, "Integrable four-dimensional symplectic maps of standard type," Phys. Lett. A **177**, 211–214 (1993).
[9] Yu. B. Suris, "A discrete-time garnier system," Phys. Lett. A **189**, 281–289 (1994).
[10] M. Bruschi, O. Ragnisco, R. M. Santini, and T. Gui-Zhang, "Integrable symplectic maps," Physica D **49**, 273–294 (1991).
[11] A. P. Fordy, "Integrable symplectic maps," in *Symmetries and Integrability of Difference Equations (Canterbury, 1996)*, edited by P. A. Clarkson and F. W. Nijhoff, London Math. Soc. Lecture Note Ser. 255 (Cambridge University Press, Cambridge, 1999), pp. 43–55.
[12] B. A. Shadwick, J. C. Bowman, and P. J. Morrison, "Exactly conservative integratos," SIAM (Soc. Ind. Appl. Math.) J. Appl. Math. **59**, 1112–1133 (1999).
[13] M. Feingold, L. P. Kadanoff, and O. Piro, "Passive scalars, 3D volume preserving maps and chaos," J. Stat. Phys. **50**, 529 (1988).
[14] A. Thyagaraja and F. A. Haas, "Representation of volume-preserving maps induced by solenoidal vector fields," Phys. Fluids **28**, 1005–1007 (1985).
[15] A. Bazzani and A. Di Sebastiano, "Perturbation theory for volume preserving maps: application to the magnetic field lines in plasma physics," in *Analysis and Modeling of Discrete Dynamical Systems*, Vol. 1 in *Adv. Discrete Math. Appl.* (Gordon and Breach, Amsterdam, 1998), pp. 283–300.
[16] R. S. MacKay, "Transport in 3D volume-preserving flows," J. Nonlinear Sci. **4**, 329–354 (1994).
[17] I. Mezic and S. Wiggins, "Nonergodicity, accelerator modes, and asymptotic quadratic-in-time diffusion in a class of volume-preserving maps," Phys. Rev. E **52**, 3215–3217 (1995).
[18] V. Rom-Kedar, L. P. Kadanoff, E. S. Ching, and C. Amick, "The break-up of a heteroclinic connection in a volume preserving mapping," Physica D **62**, 51–65 (1993).
[19] H. E. Lomelí and J. D. Meiss, "Heteroclinic primary intersections and codimension one Melnikov method for volume preserving maps," Chaos **10**, 109–121 (2000).
[20] C. Q. Cheng and Y. S. Sun, "Existence of invariant tori in three-dimensional measure-preserving mappings," Celest. Mech. Dyn. Astron. **47**, 275–292 (1990).
[21] Z. Xia, "Existence of invariant tori in volume-preserving diffeomorphisms," Ergod. Theory Dyn. Syst. **12**, 621–631 (1992).
[22] M.-Z. Qin and W.-J. Zhu, "Volume-preserving schemes and numerical experiments," Comput. Math. Appl. **26**, 33–42 (1993).
[23] Z.-J. Shang, "Construction of volume-preserving difference schemes for source-free systems via generating functions," J. Comput. Math. **12**, 265–272 (1994).
[24] F. Kang and Z. J. Shang, "Volume-preserving algorithms for source-free dynamical systems," Numer. Math. **71**, 451–463 (1995).
[25] G. R. W. Quispel, "Volume-preserving integrators," Phys. Lett. A **206**, 26–30 (1995).
[26] J. A. G. Roberts and M. Baake, "Trace maps as 3D reversible dynamical systems with an invariant," J. Stat. Phys. **74**, 829–888 (1994).
[27] M. Kohmoto, L. P. Kadanoff, and C. Tang, "Localization problem in one dimension: Mapping and escape," Phys. Rev. Lett. **50**, 1870–1872 (1983).
[28] J. A. G. Roberts, "Escaping orbits in trace maps," Physica A **228**, 295–325 (1996).
[29] D. Damanik, "Substitution Hamiltonians with bounded trace map orbits," J. Math. Anal. Appl. **249**, 393–411 (2000).
[30] H. E. Lomelí and J. D. Meiss, "Quadratic volume preserving maps," Nonlinearity **11**, 557–574 (1998).
[31] K. R. Meyer and G. R. Hall, *Introduction to the Theory of Hamiltonian Systems*, Vol. 90 in *Applied Mathematical Sciences* (Springer-Verlag, New York, 1992).